Version of Record: https://www.sciencedirect.com/science/article/pii/S2352431623000998
Manuscript_57f0b5a65fdbe1f40b7461c68a153a31

Helical dislocation in twisted bilayer graphene

Tawfiqur Rakib[1,2,*], Pascal Pochet[3], Elif Ertekin[1,2], and Harley T. Johnson[1,2,4]

[1]Department of Mechanical Science and Engineering, University of Illinois at Urbana-Champaign, Urbana IL 61801 USA
[2]Materials Research Laboratory, University of Illinois at Urbana-Champaign, Urbana IL 61801 USA
[3]Department of Physics, IriG, Univ. Grenoble-Alpes and CEA, Grenoble, France.
[4]Department of Materials Science and Engineering, University of Illinois at Urbana-Champaign, Urbana IL 61801 USA
[*]Email address: trakib2@illinois.edu

Abstract

We observe helical dislocation network in twisted bilayer graphene (tBLG), which is accompanied by large out-of-plane deformation. By atomistic calculations, we demonstrate two distinct out-of-plane deformation modes, breathing mode with small out-of-plane deformation and bending mode with one order larger corrugation magnitude compared to the breathing mode. The out-of-plane deformation is caused by inhomogeneous interlayer coupling resulting from the periodic stacking order of the tBLG moiré superlattice. Instead of commonly observed screw dislocation in tBLG, we demonstrate a slip-induced helical dislocation network in the bending mode tBLG. We show that bending mode deformation is more stable at low twist angles, as the energy savings due to interface energy exceeds the energy penalty due to the strain energy caused by the large out-of-plane deformation. Our work provides a detailed picture of a new helical dislocation structure in tBLG and establishes a

direct connection between the dislocation and deformation. Therefore, understanding the dislocation mechanics of tBLG may open up the possibility to control the corrugation, and reveal an opportunity to tune the intriguing physical properties of twisted bilayer graphene.

Keywords

Twisted bilayer graphene, Moiré superlattice, Dislocation, Corrugation, Deformation.

Recent advances in the field of 2D materials have opened up a new area of materials design in which 2D materials are stacked to create van der Waals heterostructures.[1–3] Moiré patterns appear in these heterostructures due to relative strain and rotation between the layers, and relaxation of local strain and rotation creates an inhomogeneous deformation field.[4–7] This behavior provides an opportunity to alter the electronic structure by controlling the moiré wavelength. For instance, the electronic band structure of twisted bilayer graphene (tBLG) displays flattening of bands near the Fermi level as the twist angle approaches a so-called "magic-angle" of 1.08°.[8,9] Thus, it is important to understand the mechanics behind the moiré-induced deformation field and its role in the emergence of exotic physical properties of the van der waals heterostructure. More recently, observations of correlated electronic states and unconventional superconductivity[10–13] in the magic-angle twisted bilayer graphene have further emphasized the need to gain insights into the mechanics of moiré patterns in tBLG.

In bilayer graphene, AB stacking or AC stacking (which is equivalent to BA stacking) create ground state structures with minimum potential energy among all possible stacking configurations.[14–17] However, when two layers are rotated relative to one another, a periodic variation of stacking configurations develops between the layers, creating imperfect alignment in the SP regions that separate AB and AC regions.[18,19] The SP regions of tBLG can be described, from a topological perspective, as partial dislocations of screw type.[7,20] As the twisted bilayer graphene is not in perfect AB or AC stacking configuration, it results

in an increase in the potential energy.[21–23] Within a small twist angle regime, the high potential energy of the rigid tBLG is relaxed by maximizing the area of AB/AC stacking region while reducing the area of misaligned regions of AA and SP stackings.[22,24–26] The current understanding of the relaxation is based on the in-plane relaxation of the tBLG moiré superlattice and considers a dislocation structure of pure screw character, as widely reported in the literature.[20,27] However, out-of-plane relaxation, which significantly alters the dislocation character in tBLG, is neglected in this description.[24] Since the low bending modulus of graphene[28–30] enables 3D deformation in 2D multilayer graphene through bending phenomena such as folding,[31] rippling,[32–34] and crumpling,[35] the consideration of out-of-plane relaxation in tBLG is a necessary one. Moreover, Yu et al.[36,37] have demonstrated that bending of multilayer van der Waals materials accommodates interlayer slip and dislocations. Thus, a moiré-induced out-of-plane deformation can alter the dislocation description of tBLG by accommodating dislocations other than the twist-induced screw dislocation and it is a crucial consideration for our understanding of the interfacial mechanics of tBLG.

Previous studies on out-of-plane relaxation in tBLG were based on small out-of-plane deformation, or *breathing mode*.[17,38] In 2016, Dai et al. have demonstrated large out-of-plane deformation, or *bending mode* deformation in tBLG with their continuum model and characterized the dislocation in the bending mode as a mixed dislocation. A recent study has also reported the impact of bending mode deformation on the electronic structure.[39] However, a comprehensive analysis of the dislocation mechanics of twisted bilayer graphene with large out-of-plane deformation remains necessary. In this work, we present the evidence of helical dislocations in twisted bilayer graphene related to large out-of-plane deformation in the *bending mode*. From our atomistic calculations, we also find that the bending deformation mode is more stable than the breathing mode below a certain threshold twist angle in tBLG. We attribute this stability to a reduction of the interface energy, which exceeds the energy penalty incurred by the strain energy associated with the large corrugation. Visualization of the helical dislocation core in the SP region of the tBLG also reveals the presence of interlayer

slip due to the out-of-plane deformation. We also illustrate control over the corrugation direction, indicating that the corrugation direction is dependent on the number of turns in the helix of the helical dislocation. Our study provides the first report of the presence of a helical dislocation in the tBLG moiré superlattice. Moreover, the low twist angle stability regime of the bending mode tBLG, in which we observe the helical dislocation, makes it an excellent candidate for further studies as unique electronic structure with exciting physics appears in the low twist angle regime of tBLG.[11,26,39–41]

In our study, we only analyze the case of free-standing tBLG to avoid any ambiguity that may arise due to substrate adhesion. Figure 1 illustrates three distinct types of corrugation in free-standing twisted bilayer graphene of 1.08° twist angle, as determined by our atomistic calculations (see Section 1 of the Supplementary Information for details). In the breathing mode, atoms in the AA regions of the tBLG breathing mode deform in opposite out-of-plane directions, with each layer exhibiting a corrugation magnitude of around 0.13 Å. In the bending mode, both layers of the tBLG deform in the same direction and each layer has a corrugation magnitude of 2.3 Å and 3.96 Å for the bending mode (-/-) and (+/-) cases respectively. This corrugation magnitude is determined by the difference between the maximum and minimum of the z- coordinate in each layer of the tBLG. We observe two possible cases of bending corrugation modes: bending mode (-/-) with both AA regions of the tBLG superlattice deforming in the same direction, and bending mode (+/-) with the two AA regions of the tBLG superlattice deforming in the opposite direction relative to each other, as shown in Figure 1(a). Previously, breathing mode and bending mode (+/-) tBLG were observed using a continuum-based model.[24] We note that this large out-of-plane deformation in the bending mode tBLG results in an additional radial stress in the AA regions, as depicted in Figure 3 of Ref.[39] in the case of the bending mode (-/-).

The energy density distribution in Figure 1 (b) highlights the AA, AB/AC and SP regions of the tBLG clearly. In the breathing mode tBLG, the SP region forms a triangular dislocation network that consists of three partial screw dislocations.[20,24] The dislocation line

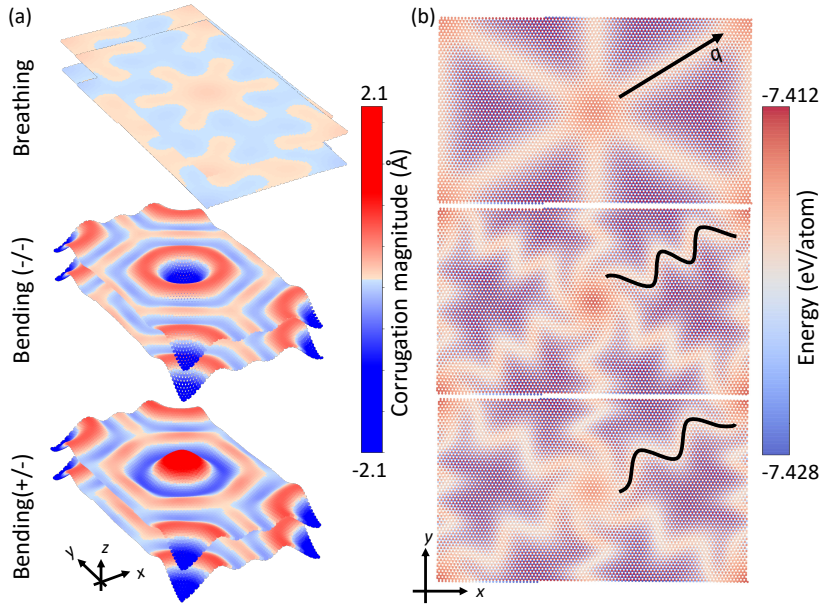

Figure 1: Corrugation in free-standing twisted bilayer graphene (tBLG) of 1.08° twist angle. (a) The 3D view of the atomic structure and the profile of the corrugation magnitude of each layer of tBLG in the breathing mode and bending modes (-/- and +/-). Compared to the bending mode cases, breathing mode tBLG shows much smaller out-of-plane displacement, or corrugation. When both AA regions of the tBLG superlattice deform in the same/opposite out-of-plane direction, we refer to the deformation as *bending mode (-/-)/bending mode (+/-)*. (b) The energy density distribution of the bottom layer of tBLG in the breathing mode and bending modes (-/- and +/-). While the SP regions in the breathing mode tBLG form straight screw dislocations, along the direction labeled q, the bending mode tBLG shows kinked sinuous dislocations. The black lines highlight the SP regions in the different corrugation modes. Here, we introduce a new coordinate system for the dislocation, where p and r axes are orthonormal to the q axis in the in-plane and out-of-plane directions.

vector along the q direction is parallel to the Burgers vector. The dislocation description in the breathing mode tBLG has been described in the literature.[7,20,24,27,42] Previous studies[34,43] have demonstrated that changing the dislocation character in vdW materials creates a change in the topological feature of the material. Therefore, a dislocation description for the bending mode tBLG needs proper analysis. In the bending mode of tBLG, the SP region deviates from the straight path, showing sinuous dislocation with wave-like features. This dislocation arises from the topological features of the tBLG in the bending mode with multiple peaks and valleys of out-of-plane deformation. A straight screw dislocation under

such large deformation would generate an unusually large interlayer shear stress.[44–46] To avoid this large stress, the interlayer dislocation in the bending mode tBLG deviates from a straight line, resulting in a sinuous dislocation in the plane of the bilayer, and minimize the total energy of the system.

Figure 2 (a) shows the energetic stability of both bending modes (-/-) and (+/-) of tBLG compared to the breathing mode by plotting the potential energy per atom with respect to AB stacked bilayer graphene of the same area. Both bending modes are found to have lower energy than the breathing mode for twist angles below 1.7°, thus establishing the upper limit of stability for bending modes. Additionally, there is very little difference in the potential energy between the two bending modes, suggesting that they are energetically degenerate.

Despite the large out-of-plane deformation in the bending modes, the energetic stability of the bending modes at low twist angle regime suggests that other effects contribute to the energetics. For instance, the interaction energy between the dislocations which depend on the dislocation density, may also have an important contribution to the energetics. The dislocation density is a measure of dislocation line length per unit volume in a 3D crystalline material. The 2D dislocation density in a tBLG moiré superlattice is dislocation line length per unit area, or $\rho \simeq \frac{4}{\sqrt{3}a}$, where a is the moiré period of the tBLG superlattice. This relationship is derived in section 2 of the supplementary information. As twist angle decreases in the tBLG superlattice, moiré period increases. Therefore, the dislocation density increases with twist angle. In the high twist angle cases, there is significant interaction energy between dislocations due to the increase in dislocation density. This interaction energy between dislocations is also included in our calculation of the total energy. We separate the energetics following Annevelink et al.[20] who have described the total energy of a bilayer graphene as –

$$E_{total} = E^{top}_{elastic} + E^{bottom}_{elastic} + E_{interface} = u + \gamma. \tag{1}$$

The total energy E_{total} is the sum of the strain energy u and the interface energy γ. The

strain energy u is the combined elastic energy of both layers of tBLG ($E^{top}_{elastic}+E^{bottom}_{elastic}$) which includes the energy contained in the strain field of the dislocation E_{el}. The interface energy γ includes the core energy of the dislocation E_{core}. So the total energy E_{total} accounts for the dislocation energy, or the sum of the energy contained in the strain field of the dislocation and the core of the dislocation. In our calculations, the strain energy u is defined as -

$$u = [E^{top}_{elastic}(r^{relaxed}) - E^{top}_{elastic}(r^{unrelaxed})] + [E^{bottom}_{elastic}(r^{relaxed}) - E^{bottom}_{elastic}(r^{unrelaxed})], \quad (2)$$

where, $r^{relaxed}$ and $r^{unrelaxed}$ are the coordinates of the relaxed and unrelaxed rigid tBLG structures respectively. The interface energy originates due to the weak van der Waals interaction between the layers, which is also represented by γ in equation 1 and is found simply by subtracting the strain energy from the total energy, $\gamma = E_{total} - (E^{top}_{elastic}+E^{bottom}_{elastic})$.

The difference in the strain energy between the bending mode and breathing mode gives us the energy penalty or saving due to the strain energy,which is calculated by -

$$\Delta u = u_{Be} - u_{Br}, \quad (3)$$

where, u_{Be} and u_{Br} are the strain energy for bending and breathing mode tBLG respectively. Similarly, we can also calculate the difference in the interface energy between bending and breathing mode tBLG, or

$$\Delta\gamma = \gamma_{Be} - \gamma_{Br}, \quad (4)$$

where, γ_{Be} and γ_{Br} are the interface energy for bending and breathing mode tBLG respectively. In Figure 2 (b), we plot the energy penalty due to the strain and interface energy in the bending mode relative to the breathing mode. We split the energy penalty into the contributions due to in-plane (xy) and out-of-plane (z) deformations. The positive/negative parts of the plot indicate the energy penalty/saving respectively. Figure 2(a) shows that

both bending modes are energetically degenerate, so we choose the case of bending mode (-/-) for our analysis in Figure 2(b). We find that the strain energy always penalizes the bending mode, as expected from the continuum description. On the other hand, the interface energy contributes to the energy saving in the bending mode compared to the breathing mode. Further examination reveals that the in-plane contribution to the interface energy also penalizes the bending mode at twist angles larger than 1.7°. However, the out-of-plane contribution of the interface energy always saves energy in the bending mode. The corrugation of a tBLG bending mode stabilizes when the energy saving is greater than the energy penalty, which occurs when the twist angle is less than 1.7°.

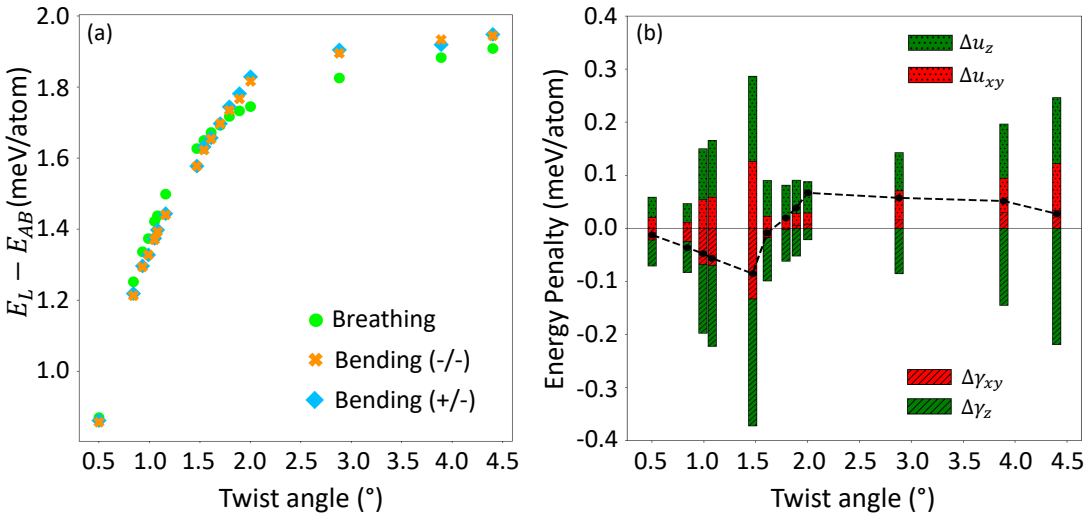

Figure 2: Energetic comparison of the deformation modes in free-standing tBLG. (a) The potential energy of the breathing and bending modes (-/- and +/-) of tBLG, with reference to the AB bilayer graphene of the same area as a function of twist angle. This shows the thermodynamic favorability of the bending mode below twist angle of approximately 1.7°. This also shows that both bending deformation modes (-/- and +/-) in tBLG are energetically degenerate. (b) Energy penalty due to the change in strain energy (Δu) and interface energy ($\Delta \gamma$) in the bending mode as a function of twist angle. The positive part of each bar indicates the energy penalty in bending mode tBLG relative to breathing mode tBLG. The negative part of the plot indicates the energy saving in bending mode tBLG relative to breathing mode tBLG. Both energy penalty and saving from the strain energy and interface energy are split into in-plane (Δu_{xy} and Δu_z) and out-of-plane ($\Delta \gamma_{xy}$ and $\Delta \gamma_z$) contributions.

The dashed lines indicate the sum of the energy penalty and saving.

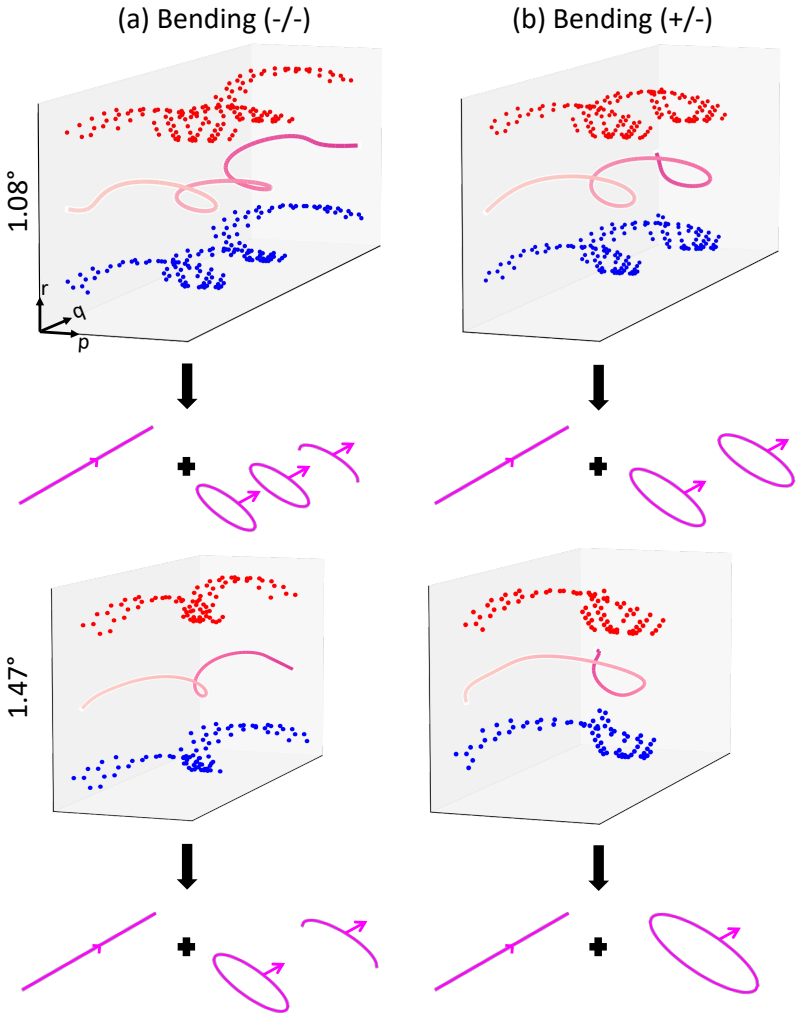

Figure 3: Helical dislocations in twisted bilayer graphene (tBLG) in both bending modes (-/- and +/-). A 3D view (Elevation angle =8° and azimuthal angle =20°) of the atomic positions in the SP regions of the (a) bending mode (-/-) and (b) bending mode (+/-) tBLG at twist angles 1.08° (Top panel) and 1.47° (Bottom panel). The colors red and blue indicate the atoms in the top and bottom graphene layers respectively. The lines between the layers of atoms indicate the position of the dislocation cores, and color intensity from light to dark purple indicates the position variation along the length of the core along the q-direction, in order to aid the 3D viewing of the helicity. The scale along the r-direction is exaggerated to reveal the helical nature of the dislocation. Each helical dislocation can be understood to be the sum of a screw dislocation and one or more edge dislocation loops,[47] as illustrated in the sketches below each panel.

To understand the energy savings in the bending mode resulting from the interfacial energy, we examine the bending mode dislocation structure, as Figure 1 (b) has shown distinct dislocation structures in the deformation modes. In Figure 3, a 3D view of the atom positions in the SP region demonstrates a helical nature of the dislocation in both bending modes. From the 2D view in Figure 1(b), it is impossible to appreciate the helical nature of the dislocation, that has been analyzed as kinked/twisted dislocation so far.[24,39] A helical dislocation is a type of mixed dislocation, comprised of a screw dislocation parallel to the axis of the helix (in the q- direction) and multiple prismatic loops of edge dislocations that have the same Burgers vector direction.[47–49] Until now, this type of helical dislocation has only been observed in three-dimensional materials.[49–53] In Figure 3, we demonstrate its presence in two-dimensional twisted bilayer graphene. We also observe that the number of turns in the helical dislocation is dependent upon the twist angle between the layers, as the number of turns decrease with an increase in the twist angle. Furthermore, when the helical dislocation connects AA regions with opposite corrugation direction, the dislocation consists of n turns and therefore contains n edge loops. In contrast, when it connects the AA regions with the same corrugation direction, it consist of $(2n+1)/2$ turns and therefore contains $(2n+1)/2$ edge loops, for all integers of n. This topological constraint in tBLG will be useful in engineering the electronic structure of the twisted bilayer graphene system.

Figure 4 presents a more in-depth analysis of the helical dislocation structure in the bending mode tBLG, showing the displacement associated with the edge dislocation loops. In Figure 4(a) and (b), we plot the displacement of the atoms in the SP region of the breathing and bending (-/-) modes along the q-direction with respect to the flat and rigid tBLG structure. While the atoms of the SP region in the breathing mode show negligble displacement along the q-direction, those in the bending mode show larger displacement. The direction of the atom displacement is opposite for atoms that are directly on top of one other. This indicates interlayer shear along the q-direction and results in an interlayer slip, as demonstrated by the dashed and dotted boxes in Figure 4 (b). Such slip is absent in

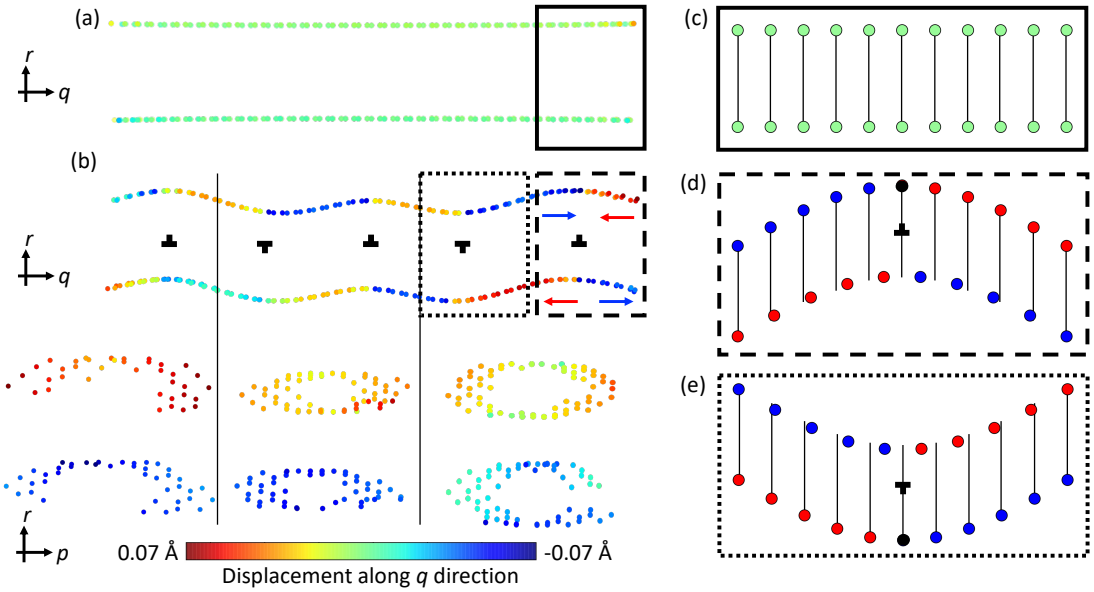

Figure 4: Illustration of the interlayer slip in the helical dislocation of tBLG. The displacement of atoms in the SP region along the q- direction for both (a) breathing mode and (b) bending mode (-/-) tBLG with respect to the unrelaxed rigid tBLG structure. The breathing mode tBLG shows negligible displacement along the q-direction compared to bending mode tBLG. Moreover, the bending mode tBLG shows opposite displacement directions in the atoms that are on top of one other, illustrating the presence of interlayer slip which forms the edge dislocation loops. In the case shown here, the atoms with positive and negative displacements form two-and-a-half loops each, as shown in the three sections of the dislocation. The sketches on the right represent atoms in the SP region within the (c) solid, (d) dashed and (e) dotted boxes, illustrating no-slip condition in the breathing mode and presence of slip in the bending modes. The sign of the edge dislocation changes as the corrugation direction changes.

breathing mode tBLG, as illustrated in the sketch in Figure 4 (c). Each interlayer slip in the SP region is associated with a dislocation loop of edge type, which has a different sign depending on the corrugation direction. These are depicted in the sketches in Figure 4 (d) and (e) to illustrate the presence of the edge dislocation in the dashed and dotted boxes of Figure 4 (b). The energetic barrier for slip in bilayer graphene is low compared to the bulk materials due to the van der Waals interaction.[15,16,19] Recent experiments and theoretical calculations have demonstrated that below a critical bending angle, bending of multilayer van der Waals materials introduces a geometrically necessary dislocation.[36,37] Similarly, the

rotation between the layers in tBLG structure introduces a geometrically necessary interlayer screw dislocations. Our study reveals that adding dislocation loops of edge type to the twist-induced screw dislocation network forms a helical dislocation network of mixed character, resulting in an elastic deformation field with large out-of-plane deformation. The addition of edge dislocation loops incurs an energetic cost; however, as the twist angle decreases and the size of the moiré superlattice increases, the interface energy of the system becomes large enough to justify the energetic cost, as illustrated in Figure 2.

When we consider both graphene layers in tBLG, we find origins of the dislocations loops in the atoms of positive and negative displacements, as illustrated in Figure 4 (b). Each edge dislocation is composed of a half loop of atoms with positive displacement and half a loop of atoms with negative displacement. In the bending mode (-/-) tBLG case, we observe two-and-a-half loops of atoms with positive displacement and the same number of loops of atoms with negative displacement, corresponding to the two-and-a-half turns of the dislocation helix, as depicted in Figure 3 (a). The same interlayer slip and edge dislocation loops are observed in the bending mode (+/-) case, which is illustrated in Figure S1 of the supplementary information. In this case, there are two dislocation loops for the atoms with positive and negative displacement, as there are two turns of the helical dislocation.

Our results have significant implications for the mechanical and electronic properties of twisted bilayer graphene. Until now, the current understanding of dislocation structure in tBLG has been based on the pure screw dislocation character that accompanies a small out-of-plane deformation (breathing mode). However, we demonstrate that a helical dislocation in tBLG results in an elastic deformation field with large out-of-plane deformation (consistent with the known bending deformation mode), enabling 3D deformation in 2D materials. The helical dislocation is formed by the combination of dislocation loops of edge character and the twist-induced screw dislocation. We also show that below a transition twist angle, the largely corrugated tBLG structure in the bending mode becomes energetically stable due to the stress-relief caused by the interface energy. But we also note that transition twist

angle and the large deformation are generally affected by thermal effects[54,55] and presence of a substrate.[56] Furthermore, the energy barrier imposed in our calculation to obtain bending modes tBLG is significantly smaller than the value of kT at room temperature. Thus, increasing the temperature of a tBLG system may create thermal effects that can overcome the energy barrier between the breathing and bending modes. The presence of a substrate does not change the transition twist angle, but does reduce the out-of-plane deformation magnitude in tBLG, as reported in our recent work.[39] Our recent work[39] has also demonstrated that such large corrugation in tBLG explains the presence of several electronic effects at the single particle level, such as symmetry breaking and pseudogap states, which can not be explained by small corrugation. Our new findings indicate that the large corrugation in tBLG is driven by the elastic deformation field of the helical dislocation. This suggests a link between the helical dislocation and the emergence of exciting electronic properties in tBLG such as unconventional superconductivity,[11] electron correlations,[10,40] and ferromagnetism.[57]

Data availability

The data that support the findings of this study are available through a Github repository managed by the authors.

Acknowledgements

TR, EE, and HTJ acknowledge the U.S. Department of Energy, Office of Science, Office of Basic Energy Sciences, Computational Materials Sciences program under Award Number DE-SC0020177. This research used resources of the Oak Ridge Leadership Computing Facility, which is a DOE Office of Science User Facility supported under Contract DE-AC05-00OR22725. TR acknowledges the help from Professor Matthew Turk and Dr. Chris Havlin for helping with the visualization of the helical dislocations.

Author contributions

TR developed the work-flow for the project, performed the simulations, investigated the results, and prepared the manuscript. HTJ and EE administered the project and acquired the funds that supported the research. HTJ, EE and PP supervised the project and reviewed the manuscripts. All authors contributed to this work.

Competing Interests

The authors declare no competing interests.

References

[1] Geim, A. K. & Grigorieva, I. V. Van der waals heterostructures. *Nature* **499**, 419–425 (2013).

[2] Haigh, S. J. *et al.* Cross-sectional imaging of individual layers and buried interfaces of graphene-based heterostructures and superlattices. *Nature Mater* **11**, 764–767 (2012). URL `https://www.nature.com/articles/nmat3386`.

[3] Dean, C. *et al.* Graphene based heterostructures. *Solid State Communications* **152**, 1275–1282 (2012).

[4] Van Wijk, M., Schuring, A., Katsnelson, M. & Fasolino, A. Moiré patterns as a probe of interplanar interactions for graphene on h-bn. *Physical review letters* **113**, 135504 (2014).

[5] Hermann, K. Periodic overlayers and moiré patterns: theoretical studies of geometric properties. *Journal of Physics: Condensed Matter* **24**, 314210 (2012).

[6] Van Wijk, M., Schuring, A., Katsnelson, M. & Fasolino, A. Relaxation of moiré patterns for slightly misaligned identical lattices: graphene on graphite. *2D Materials* **2**, 034010 (2015).

[7] Pochet, P., McGuigan, B. C., Coraux, J. & Johnson, H. T. Toward Moiré engineering in 2D materials via dislocation theory. *Applied Materials Today* **9**, 240–250 (2017).

[8] Suárez Morell, E., Correa, J. D., Vargas, P., Pacheco, M. & Barticevic, Z. Flat bands in slightly twisted bilayer graphene: Tight-binding calculations. *Phys. Rev. B* **82**, 121407 (2010). URL `https://link.aps.org/doi/10.1103/PhysRevB.82.121407`.

[9] Bistritzer, R. & MacDonald, A. H. Moiré bands in twisted double-layer graphene. *Proceedings of the National Academy of Sciences* **108**, 12233–12237 (2011). URL `https://www.pnas.org/doi/abs/10.1073/pnas.1108174108`.

[10] Cao, Y. *et al.* Tunable correlated states and spin-polarized phases in twisted bilayer–bilayer graphene. *Nature* **583**, 215–220 (2020).

[11] Cao, Y. *et al.* Unconventional superconductivity in magic-angle graphene superlattices. *Nature* **556**, 43–50 (2018). URL `https://www.nature.com/articles/nature26160`. Number: 7699 Publisher: Nature Publishing Group.

[12] Wong, D. *et al.* Cascade of electronic transitions in magic-angle twisted bilayer graphene. *Nature* **582**, 198–202 (2020).

[13] Uri, A. *et al.* Mapping the twist-angle disorder and landau levels in magic-angle graphene. *Nature* **581**, 47–52 (2020).

[14] Lu, C. *et al.* Low-energy electronic properties of the ab-stacked few-layer graphites. *Journal of Physics: Condensed Matter* **18**, 5849 (2006).

[15] Zhou, S., Han, J., Dai, S., Sun, J. & Srolovitz, D. J. van der waals bilayer energetics: Generalized stacking-fault energy of graphene, boron nitride, and graphene/boron nitride bilayers. *Physical Review. B, Condensed Matter and Materials Physics* **92** (2015).

[16] Dai, Z., Liu, L. & Zhang, Z. Strain Engineering of 2D Materials: Issues and Opportunities at the Interface. *Advanced Materials* **31** (2019). URL `https://onlinelibrary.wiley.com/doi/abs/10.1002/adma.201805417`.

[17] Uchida, K., Furuya, S., Iwata, J.-I. & Oshiyama, A. Atomic corrugation and electron localization due to moiré patterns in twisted bilayer graphenes. *Phys. Rev. B* **90**, 155451 (2014). URL `https://link.aps.org/doi/10.1103/PhysRevB.90.155451`. Publisher: American Physical Society.

[18] Hattendorf, S., Georgi, A., Liebmann, M. & Morgenstern, M. Networks of aba and abc stacked graphene on mica observed by scanning tunneling microscopy. *Surface science* **610**, 53–58 (2013).

[19] Alden, J. S. *et al.* Strain solitons and topological defects in bilayer graphene. *Proceedings of the National Academy of Sciences* **110**, 11256–11260 (2013). URL `https://www.pnas.org/doi/abs/10.1073/pnas.1309394110`.

[20] Annevelink, E., Johnson, H. T. & Ertekin, E. Topologically derived dislocation theory for twist and stretch moiré superlattices in bilayer graphene. *Phys. Rev. B* **102**, 184107 (2020). URL `https://link.aps.org/doi/10.1103/PhysRevB.102.184107`.

[21] Jain, S. K., Juričić, V. & Barkema, G. T. Structure of twisted and buckled bilayer graphene. *2D Materials* **4**, 015018 (2016).

[22] Zhang, K. & Tadmor, E. B. Structural and electron diffraction scaling of twisted graphene bilayers. *Journal of the Mechanics and Physics of Solids* **112**, 225–238 (2018).

[23] Rakib, T., Pochet, P., Ertekin, E. & Johnson, H. T. Moiré engineering in van der waals heterostructures. *Journal of Applied Physics* **132**, 120901 (2022).

[24] Dai, S., Xiang, Y. & Srolovitz, D. J. Twisted Bilayer Graphene: Moiré with a Twist. *Nano Lett.* **16**, 5923–5927 (2016). URL `https://doi.org/10.1021/acs.nanolett.6b02870`.

[25] Gargiulo, F. & Yazyev, O. V. Structural and electronic transformation in low-angle twisted bilayer graphene. *2D Mater.* **5**, 015019 (2017). URL `https://doi.org/10.1088/2053-1583/aa9640`. Publisher: IOP Publishing.

[26] Yoo, H. *et al.* Atomic and electronic reconstruction at the van der Waals interface in twisted bilayer graphene. *Nat. Mater.* **18**, 448–453 (2019). URL `https://www.nature.com/articles/s41563-019-0346-z`. Number: 5 Publisher: Nature Publishing Group.

[27] Gornostyrev, Y. N. & Katsnelson, M. Origin of the vortex displacement field in twisted bilayer graphene. *Physical Review B* **102**, 085428 (2020).

[28] Behfar, K., Seifi, P., Naghdabadi, R. & Ghanbari, J. An analytical approach to determination of bending modulus of a multi-layered graphene sheet. *Thin Solid Films* **496**, 475–480 (2006).

[29] Lu, Q., Arroyo, M. & Huang, R. Elastic bending modulus of monolayer graphene. *Journal of Physics D: Applied Physics* **42**, 102002 (2009).

[30] Chen, S. & Chrzan, D. Continuum theory of dislocations and buckling in graphene. *Physical Review B* **84**, 214103 (2011).

[31] Chen, X., Yi, C. & Ke, C. Bending stiffness and interlayer shear modulus of few-layer graphene. *Applied Physics Letters* **106**, 101907 (2015).

[32] Bao, W. *et al.* Controlled ripple texturing of suspended graphene and ultrathin graphite membranes. *Nature nanotechnology* **4**, 562–566 (2009).

[33] Zhao, P. *et al.* Geometry and chiral symmetry breaking of ripple junctions in 2d materials. *Journal of the Mechanics and Physics of Solids* **131**, 337–343 (2019).

[34] Kushima, A., Qian, X., Zhao, P., Zhang, S. & Li, J. Ripplocations in van der waals layers. *Nano letters* **15**, 1302–1308 (2015).

[35] Zang, J. *et al.* Multifunctionality and control of the crumpling and unfolding of large-area graphene. *Nature materials* **12**, 321–325 (2013).

[36] Han, E. *et al.* Ultrasoft slip-mediated bending in few-layer graphene. *Nature materials* **19**, 305–309 (2020).

[37] Yu, J. *et al.* 2d materials: Designing the bending stiffness of 2d material heterostructures (adv. mater. 9/2021). *Advanced Materials* **33**, 2170066 (2021).

[38] Lucignano, P., Alfè, D., Cataudella, V., Ninno, D. & Cantele, G. Crucial role of atomic corrugation on the flat bands and energy gaps of twisted bilayer graphene at the magic angle θ 1.08°. *Physical Review B* **99**, 195419 (2019).

[39] Rakib, T., Pochet, P., Ertekin, E. & Johnson, H. T. Corrugation-driven symmetry breaking in magic-angle twisted bilayer graphene. *Communications Physics* **5**, 1–7 (2022).

[40] Kerelsky, A. *et al.* Maximized electron interactions at the magic angle in twisted bilayer graphene. *Nature* **572**, 95–100 (2019). URL `https://www.nature.com/articles/s41586-019-1431-9`. Number: 7767 Publisher: Nature Publishing Group.

[41] Xie, M. & MacDonald, A. H. Nature of the correlated insulator states in twisted bilayer graphene. *Physical review letters* **124**, 097601 (2020).

[42] Dai, S., Xiang, Y. & Srolovitz, D. J. Structure and energetics of interlayer dislocations in bilayer graphene. *Physical Review B* **93**, 085410 (2016).

[43] Liu, Y. *et al.* Helical van der waals crystals with discretized eshelby twist. *Nature* **570**, 358–362 (2019).

[44] Han, Y. *et al.* Geometric frustration in buckled colloidal monolayers. *Nature* **456**, 898–903 (2008).

[45] Kang, S. H. *et al.* Complex ordered patterns in mechanical instability induced geometrically frustrated triangular cellular structures. *Physical review letters* **112**, 098701 (2014).

[46] Bhandakkar, T. K. & Johnson, H. T. Diffusion induced stresses in buckling battery electrodes. *Journal of the Mechanics and Physics of Solids* **60**, 1103–1121 (2012).

[47] Hull, D. & Bacon, D. J. *Introduction to dislocations*, vol. 37 (Elsevier, 2011).

[48] Weertman, J. Helical dislocations. *Physical Review* **107**, 1259 (1957).

[49] Amelinckx, S., Bontinck, W., Dekeyser, W. & Seitz, F. On the formation and properties of helical dislocations. *Philosophical Magazine* **2**, 355–378 (1957).

[50] Jones, D. & Mitchell, J. Observations on helical dislocations in crystals of silver chloride. *Philosophical Magazine* **3**, 1–7 (1958).

[51] Caslavsky, J. L. & Gazzara, C. P. The observation of helical dislocations in sapphire. Tech. Rep., ARMY MATERIALS AND MECHANICS RESEARCH CENTER WATERTOWN MA (1971).

[52] Haley, J. *et al.* Helical dislocations: Observation of vacancy defect bias of screw dislocations in neutron irradiated fe–9cr. *Acta Materialia* **181**, 173–184 (2019).

[53] Horibuchi, K., Yamaguchi, S., Kimoto, Y., Nishikawa, K. & Kachi, T. Formation of helical dislocations in ammonothermal gan substrate by heat treatment. *Semiconductor Science and Technology* **31**, 034002 (2016).

[54] Gao, W. & Huang, R. Thermomechanics of monolayer graphene: Rippling, thermal expansion and elasticity. *Journal of the Mechanics and Physics of Solids* **66**, 42–58 (2014).

[55] Yan, W., Shui, L., Ouyang, W. & Liu, Z. Thermodynamic model of twisted bilayer graphene: Entropy matters. *Journal of the Mechanics and Physics of Solids* **167**, 104972 (2022).

[56] Chang, Z., Yang, R. & Wei, Y. The linear-dependence of adhesion strength and adhesion range on temperature in soft membranes. *Journal of the Mechanics and Physics of Solids* **132**, 103697 (2019).

[57] Sharpe, A. L. *et al.* Emergent ferromagnetism near three-quarters filling in twisted bilayer graphene. *Science* **365**, 605–608 (2019).

Declaration of interests

☒ The authors declare that they have no known competing financial interests or personal relationships that could have appeared to influence the work reported in this paper.